

Using Network Reliability to Understand International Food Trade Dynamics

Madhurima Nath^{1,2}, Srinivasan Venkatramanan¹, Bryan Kaperick^{1,4}, Stephen Eubank^{1,2,3}, Madhav V. Marathe^{1,5}, Achla Marathe^{1,6}, and Abhijin Adiga¹

Abstract. As modern society increasingly relies on long-distance agricultural trade, food networks act as conduits for invasive species spread, contamination and other disruptions. Therefore, understanding their structural and dynamical properties is critical for food security and social welfare. Here, we present a novel approach to identify important dynamics-induced clusters of highly-connected nodes in the network. The method employs Moore-Shannon network reliability coupled with discrete-time SIR diffusion model over directed weighted networks. We apply it to analyze international trade networks corresponding to four solanaceous crops obtained using the Food and Agricultural Organization trade database.

Our analysis shows that the structure and dynamics can greatly vary across commodities. However, a consistent pattern that we observe in these commodity-specific networks is that almost all clusters that are formed are between adjacent countries in regions where liberal bilateral trade relations exist. Our analysis of networks of different years shows that intensification of trade has led to increased size of clusters, which in turn implies that the number of countries spared from the network effects of disruption is reducing. Finally, applying this method to the aggregate network obtained by combining the four networks reveals clusters very different from those found in the constituent networks.

1 Introduction

The global food system is characterized by concentrated and specialized agricultural production, and an ever increasing reliance on the long-distance trade of these com-

¹Network Dynamics and Simulation Science Laboratory, Biocomplexity Institute,²Department of Physics,³Department of Population Health Sciences,⁴Department of Mathematics,⁵Department of Computer Science,⁶Department of Agricultural and Applied Economics, Virginia Tech, Blacksburg, VA, 24061, USA

e-mail: {mnath,vsrniv,bryanjk,eubank,mmarathe,amarathe,abhijin}@vt.edu

modities. This makes it vulnerable to extreme events such as climate change [16], invasive species introductions [9] and contamination [5]. Therefore, understanding the structural and dynamical properties of food trade networks is critical to ensure food security, health and economic stability.

Here, we study international agricultural commodity networks, where the network consists of countries as nodes and directed weighted edges representing the volume of export from the source to the destination. In particular, we analyze a set of commodity-specific networks comprising of crops belonging to the *Solanaceae* family, which includes tomato, eggplant, potato and peppers over a span of 10 years. These networks are constructed from the Food and Agricultural Organization (FAO) trade matrix database [6]. Previous works [1, 5, 17], have typically studied networks aggregated over multiple commodities. However, there are several applications where it is important to consider commodity-specific trade.

Our choice of networks of solanaceous crops is motivated by the recent global invasion of the pest, South American tomato leafminer or *Tuta absoluta* [2, 3]. Within a decade of its accidental introduction to Spain from its native habitat in South America, this moth has spread to most parts of Europe and Africa, West, Central and South Asia. There is overwhelming evidence that it has spread to extensive trade between countries in these regions. While its primary target is tomato, it can attack and survive on other solanaceous crops such as the ones mentioned above. In general, there is an emerging trend to account for trade and other human-mediated pathways while modeling invasive species spread [8]. Besides, independent of this application there is merit in analyzing flows of these crops; tomato and potato are among the top traded essential vegetables. Disruptions in their production or supply can have enormous socio-economic impact. This analysis will help identify the vulnerabilities in these networks and help risk analysts make informed decisions in mitigating contagion processes over these networks.

Our contributions. In this paper, we develop a novel method to analyze the dynamical properties of the above-mentioned networks. Through the lens of a discrete-time SIR process coupled with network reliability principles [12, 20], we identify critical subsets of nodes in the networks, which we refer to as *contagion clusters* (formal definitions are provided later). Broadly, these are well-connected maximal subsets of nodes such that if the infection is introduced to the cluster, it spreads rapidly within the cluster. We assess their vulnerability and role as hubs by computing the minimum (weight) cuts and total volumes of their imports and exports with the rest of the network. Further, we compare the networks based on their contagion clusters: How do the networks and therefore the contagion clusters differ across communities? How have they evolved over time? How does an aggregated network differ from its constituent networks? Some of our results are as follows:

- We identified important contagion clusters in the food networks which act as hubs towards the spread of contagion; they are not only vulnerable to attacks, but can also spread the infection to a large number of vertices.

- We observe that the size and participating vertices of prominent contagion clusters can differ greatly across commodities. However, all of these clusters tend to be region-specific, e.g., countries localized to Europe or North America.
- Our analysis of the tomato networks over a period of 10 years reveals that intensification of trade has led to increase in both volume traded within contagion clusters and their connectivity outside. Moreover, the size of top contagion clusters has increased over the years.
- Some contagion clusters in the aggregate network span continents, unlike those in the commodity-specific networks.

Methodologically, we provide a novel way to find decompose and analyze directed weighted networks.

Related work. A number of works have analyzed world trade networks constructed from UN datasets. Serrano and Boguná [17] analyze the structural properties of the World Trade Web obtained by aggregated trade statistics from the ComTrade dataset. Baskaran et al. [1] study the evolution of networks induced by different product groups over time. Perhaps, the work that is closest to ours is by Ercsey et al. [5]. In this paper, an international food trade network is constructed by aggregating product codes corresponding to food. They perform structural analysis based on weighted betweenness centrality and graph density, and dynamical analysis using a diffusion model to assess the complexity and vulnerabilities of the network. There are two key differences between the above-mentioned works and ours. Unlike the FAOSTAT trade matrix, ComTrade reports the value of goods exported from one country to another in US dollars. Secondly, the network is obtained by aggregating categories corresponding to food products. Suweis et al. [18] use production and trade data from FAO and demographics information to assess the resilience and the reactivity of the coupled population food system. To this end, they develop a diffusion model referred to as food-demographic delayed logistic model. Again, they use aggregated trade data for network construction.

Agricultural commodity networks are being increasingly considered in specific application domains such as invasive species spread, bio-warfare and transportation. Nopsa et al. [8] study rail networks of grain transport in the US and Australia in the context of pathogen and mycotoxin spread. They identify key nodes in the network to monitor or quarantine so that the spread is mitigated. Venkatramanan et al. [19] model the domestic seasonal vegetable trade network in Nepal and show that spread of invasive species is correlated with trade flows of host crops. Robinson et al. [15] consider the network of US food flows, and use a linear programming approach to reconfigure the flows to minimize total miles in the network.

Community detection in unweighted, undirected networks has been studied extensively using algorithms based on modularity [13], q-state Potts model [14], extremal optimization of modularity [4]. Malliaros et al. [10] have explored clustering for directed networks. Ghosh et al. [7] have examined the dependence of a dynamic process on the structure of the network to identify important vertices participating in the dynamics and communities in the network.

2 Network construction

The international food trade networks that we study in this paper are obtained from Food and Agriculture Organization (FAO) [6]. Especially, we obtained the Detailed Trade Matrices at the country level for each of the crops (Tomatoes, Potatoes, Eggplants and Peppers) and years (2005-2013) of interest. We also focused on the *Quantity* of trade (measured in tonnes) and not the associated monetary *Value* (measured in US dollars). The raw data is structured as follows for each year Y and crop C : Given a pair of countries (r, p) (stands for *Reporter* and *Partner*), we have two quantities namely $E_{r,p}$ and $I_{r,p}$. $E_{r,p}$ is the quantity of the commodity being exported by r to p as reported by r . Likewise, $I_{r,p}$ is the quantity of the commodity being imported by r from p , as reported by r .

We note that there are reporting discrepancies in the raw data, i.e., $E_{r,p} \neq I_{p,r}$ for some pairs of (r, p) . So we construct a *maximal* trade matrix whose edge weights are given by $W_{i,j}$ as

$$W_{i,j} = \max(E_{i,j}, I_{j,i}).$$

In the context of food security and invasion risk, the maximal trade matrix can be considered as the worst-case scenario.

3 Network reliability and contagion clusters

Network reliability was originally proposed by Moore and Shannon [11] to understand the reliability of electrical circuits with unreliable individual components. Recently [12, 20], this concept has been adapted to understand the likelihood of certain events (aka *properties*) occurring in graph-based dynamical systems. We introduce basic terminology and associated notations to describe the concepts and our algorithm to discover contagion clusters in this section.

Given a graph $\mathcal{G} = (V, E)$, and dynamics \mathcal{D} , reliability $R(\mathcal{G}, \mathcal{D}, \mathcal{P})$ is used to denote the probability of property \mathcal{P} being satisfied by the dynamic process. Here, \mathcal{D} is the independent cascade epidemic process or the discrete-time Susceptible-Infected-Removed (SIR) process where an infected node remains in that state for one unit step before transitioning to R. One possible \mathcal{P} could be the property that at least α fraction of nodes are infected. Note that for contagion-like dynamics on graphs, a typical parameter associated with it is the probability of transmission through each edge x . When the property of interest is implicitly understood, the reliability (polynomial) is sometimes expressed as $R(x; \mathcal{G})$, and is a global measure which depends on both the network structure and the dynamics.

Independent cascade process can be viewed as the random subgraph obtained by sampling edges in \mathcal{G} independently with probabilities x , thus resulting in a contagion subgraph \mathcal{G}_x . \mathcal{G}_x may or may not satisfy the property \mathcal{P} of interest. Let *struts* be the minimal subgraphs that satisfy property \mathcal{P} . Likewise, let *cuts* be minimal subgraphs

which when removed from \mathcal{G} destroy the property \mathcal{P} . Together, we denote them as *cruxes*.

Remark: Network reliability calculation for homogeneous edge probabilities is mathematically and computationally more amenable than for arbitrary edge weights. Hence for the purpose of computing $R(x; \mathcal{G})$, we convert the maximal trade matrix weights into parallel edges. Given a step size Δ , an edge of weight w between nodes i and j is converted into $\lfloor \frac{w}{\Delta} \rfloor$ simple edges between them. This also allows us to (a) quantize the flow volume to separate edges representing individuals shipments, (b) evaluate the impact of reducing edge weights, instead of completely removing them and (c) simulate unweighted version of the dynamics where each simple edge has an associated probability of x . The resulting multi-graph \mathcal{G} is then the quantized representation of the maximal trade matrix W .

Contagion Clusters Extraction Algorithm. In \mathcal{G} , we are interested in collections of nodes $\{CC_i\}$ which have a shared vulnerability to the contagion, i.e., infection of a node $i \in CC_i$ significantly increases the likelihood of other nodes $j \in CC_i$ to be infected. Though similar to the concept of communities, note that there is an added emphasis on the dynamics. We refer to these as *contagion clusters*. The necessary characteristic of a contagion cluster is that it must induce a strongly connected component (SCC) in the network. In addition, the connectivity within the cluster should be strong enough for each vertex to have enough influence on the rest of the nodes in the cluster. We develop an algorithm called **COCLEA (COntagion CLusters EXtraction Algorithm)** to identify these clusters using network reliability.

Definition: Given a network \mathcal{G} , the *contagion score* of a set $X \subseteq V$ is given as:

$$\psi(X) = \frac{1}{|X|} \sum_{i \in X} \sigma_x^{\mathcal{D}}(i)$$

where $\sigma_x^{\mathcal{D}}(i)$ is the expected number of nodes in X that get infected by dynamics \mathcal{D} , when we start by initially infecting i with transmission probability, x . A set X is a *contagion cluster* of size n , if it maximizes $\psi(X)$ for all $X \subseteq V$ with $|X| = n$.

The algorithm for extracting mutually exclusive contagion clusters (or potential candidates) of size $\leq n$ is described in Algorithm 1. The property \mathcal{P} of interest is that there exists no strongly connected component (SCC) with $|SCC| > n$, where n is a parameter that governs maximum contagion cluster size. The edge ranking algorithm scores each edge by its marginal contribution to the overall reliability. The contribution of an edge e is estimated as follows: Draw a random sample of cruxes $K = \{k\}$, and identify the subset of cruxes that do not contain e , i.e., $K'_e = \{k : e \notin k\}$. The inverse of the probability that at least one of these cruxes occur in a random subgraph of \mathcal{G} is the score $\eta_x(e)$. Let $\max |SCC|$ be the size of the largest strongly connected component in \mathcal{G} . When $\max |SCC| > n$, edges are removed sequentially by importance until there exists no SCC with $|SCC| > n$. If $\max |SCC| \leq n$, the algorithm terminates and returns all contagion clusters at that stage. Note that in the process of detecting such clusters, we also rank the edges in \mathcal{G} in terms of their importance for the contagion process.

Remark on edge score: The more likely it is that a random edge would show up in a certain set of cruxes, the less likely it is that an edge that shows up in that set is important. Hence an edge present in a single small crux is more important than an edge that is present in a single larger crux. Similarly, an edge that is present in many cruxes is more important than one that is present in only a few (if their sizes are all the same).

Algorithm 1: Contagion Clusters Extraction Algorithm (COCLEA)

Result: edge rankings ER ; contagion clusters $\{CC_l\}$

```

1  $\mathcal{G} = (V, E); ER = [];$ 
2 while  $\mathcal{G}$  does not satisfy  $\mathcal{P}$  do
3   Randomly sample cruxes  $K = \{k\};$ 
4   For every  $e \in E(\mathcal{G}), \eta_x(e) = \mathbb{P}[\exists k' \in K'_e : k' \subseteq \mathcal{G}_x]^{-1};$ 
5    $e^* = \arg \max_e \eta_x(e);$ 
6    $ER = ER \cup \{e^*\};$ 
7    $E(\mathcal{G}) = E(\mathcal{G}) \setminus e^*;$ 
8 end
9  $\{CC_l\} =$  strongly connected components in  $\mathcal{G}$ 

```

4 Experimental results

The clustering algorithm was applied to study annual trade networks corresponding to four major crops of the *Solanaceae* family: tomato, potato, eggplant and pepper between 2005 and 2013 (Table 1). We discovered the contagion clusters for each of these networks, the prominent ones are listed in Table 2. In this section, we study the properties of these clusters and compare them across commodities and years. For the three input parameters of COCLEA, we used the following values: cluster size ($n = 2, 5, 10, 20, 30, |V|$), step size ($\Delta = 1000$) and probability ($p = 0.01, 0.1, 0.5$). Also, throughout this section, for brevity, we refer to countries by their ISO-3 code.

Table 1: Networks and their properties.

Network	Nodes	Edges	Volume (Kilo Ton.)	Network	Nodes	Edges	Volume (Kilo Ton.)
Tom05	186	1198	5355	Egg05	142	656	346
Tom07	189	1310	7360	Egg07	149	715	440
Tom09	188	1200	7490	Egg09	146	681	458
Tom11	192	1249	7822	Egg11	146	739	490
Tom13	189	1305	8247	Egg13	160	776	487
Pot05	206	1561	10156	Pep05	184	1809	330
Pot07	204	1780	12417	Pep07	188	1973	350
Pot09	204	1657	11659	Pep09	183	1804	348
Pot11	205	1778	14239	Pep11	183	1912	367
Pot13	205	1834	14575	Pep13	192	2063	412

Table 2: Prominent/interesting contagion clusters. All volumes are in Kilo Tonnes. Regarding network names, “NA” stands for North America.

Cluster name	Countries	Network	Num. edges	Vol.	Min. wt.	Min. cut	Inc. nbrs	Inc. vol.	Outg. nbrs	Outg. vol.
EU-T-13	PRT, NLD, BEL, FRA, ESP	Tom13	20	691	32	3	47	421	78	2142
EU-T-11	”	Tom11	20	705	44	3	46	400	68	1949
EU-T-09	”	Tom09	21	658	31	3	41	447	69	1755
EU-T-07	”	Tom07	20	646	28	2	48	371	70	1650
EU-T-05	”	Tom05	20	580	23	2	52	309	90	1567
NA-T-13	USA, MEX, CAN	Tom13	6	1955	15	1	23	21	43	12
NA-T-11	”	Tom11	6	1858	23	1	28	25	36	9
NA-T-09	”	Tom09	6	1604	57	1	25	17	35	4
NA-T-07	”	Tom07	6	1522	48	1	22	13	43	8
NA-T-05	”	Tom05	6	1265	14	1	26	13	33	7
C1-P-13	FRA, BEL, DEU, ISR	NLD, Pot13	20	4913	53	4	43	385	145	3773
C2-P-13	FRA, EGY, ITA, GBR, ESP, NLD, ISR	BEL, DNK, Pot13	87	7602	53	6	52	249	147	248
SE-P-13	MYS, SGP, IDN	Pot13	6	14	2	2	28	290	13	2
SA-P-13	LKA, IND, VNM	Pep13	5	17	1	1	35	19	122	166

To quantify the structural properties of the clusters and compare one another we computed different metrics for each mined cluster. This is summarized in Table 2 for some of the chosen clusters. To assess the strength of connectivity among cluster vertices, we computed minimum weighted cut and the minimum cut of the cluster by applying the max-flow min-cut algorithm on the weighted and unweighted network induced by the cluster. The minimum weighted cut gives the minimum total volume of trade that needs to be reduced in order to disconnect the cluster, i.e., it will no longer be a strongly connected component. The minimum cut gives the minimum number of edges that need to be removed to disconnect the cluster. To assess a cluster’s role in the bigger network that it is part of, we also looked at the total volume of import into the cluster (*incoming volume*) and total volume of export from the cluster (*outgoing volume*). The former is an indicator of vulnerability of the cluster to attacks, while the latter indicates the influence the cluster has on the rest of the network. We also computed the number of distinct *in-neighbors* and *out-neighbors* of the cluster. An in-neighbor (out-neighbor) is a node which does not belong to the cluster and has an outgoing (incoming) edge to (from) the cluster.

Contagion clusters in commodity specific networks. Fig 1 show the contagion clusters for tomato and potato trade networks when $\Delta = 1000$ and n is restricted to 20. The colored clusters on the right of both the figures denote the contagion clusters obtained using COCLEA. The big cluster on the left represent countries which do not belong to any such SCC. However, they are either connected to some

countries in the left cluster itself or to some of the countries outside. The colored edges connect countries belonging to corresponding colored cluster.

We observe that for tomato networks, the European countries form a strong cluster and is separated from others. However, in the case of potatoes, the European countries have strong trading relations with both African and West Asian countries (C1-P-13 and C2-P-13 for example). The North American countries (NA-T-13) are fairly isolated from the rest of the world. Among the European countries, the core countries correspond to EU-T-13 (Table 2). The European clusters, unlike the North American cluster have lot more incoming and outgoing neighbors as well as volume. This indicates that not only is this cluster more vulnerable to attacks, it is also a big hub and can lead to rapid spread of contagion to other several countries. Another interesting difference between tomato and potato networks is the existence of several smaller clusters compared to tomato networks (e.g., SE-P-13).

In general, the eggplant network is very similar to that of the tomato network. However, the volumes of trade are much small. While the EU-T-13 cluster appears here, among the North American countries, only the cluster (USA, CAN) appears. The most distinct of all networks is that of peppers (Pep13). It has only one cluster (SA-P-13).

Effect of cluster size. Fig 2 shows how the largest SCC in a network decomposes into smaller clusters as we decrease the parameter n . Consider network Tom13 quantized with $\Delta = 1000$. The last row represents the largest strongly connected component obtained for all $n > 21$, and consists solely of European countries. As we decrease n , note that smaller clusters such as (SVN, HRV), (CZE, SVK), (HUN, ROU) separate out at fairly early stages. Also countries like GRC and BGR drop out of any strongly connected components (shown in grey). For smaller n , we see the emergence of sub-clusters among Western European nations such as (GBR, IRL) and the (ESP, PRT), etc. Alternatively for potato network with $\Delta = 10000$, we see emergence of inter-continent clusters such as (EGY, GBR), and the presence of ISR in the largest SCC for most values of n .

Network evolution over time. We studied the evolution of the cluster structure over time. Due to lack of space, we only present the results for the tomato networks. Overall, some clusters have remained stable over time. Two of them that stand out are the core European cluster (EU-T-*) and the North American triple (NA-T-*) (see Table 2). However, trade within these clusters has intensified over the years. Also, both the incoming and outgoing volume have increased considerably. While the number of countries to which these countries export has increased in the case of NA-T-*, the number of countries from which this cluster imports has generally remained same. Other clusters which appear for all years are (NZL, AUS) and (ARE, OMN). In the recent years, new clusters have formed (THA, MYS) in Southeast Asia and (ZAF, NAM) in Southern Africa. In fact, both these clusters export to a large number of countries (43 and 23 respectively). There are some clusters (SYR, JOR, LBN, SAU) which appear only in 2007 and earlier networks. Perhaps, political conditions have led to a decrease or pause in trade between them.

The effect of aggregation. While in the commodity-specific networks, all major clusters that were discovered were mostly region-specific, in the aggregated net-

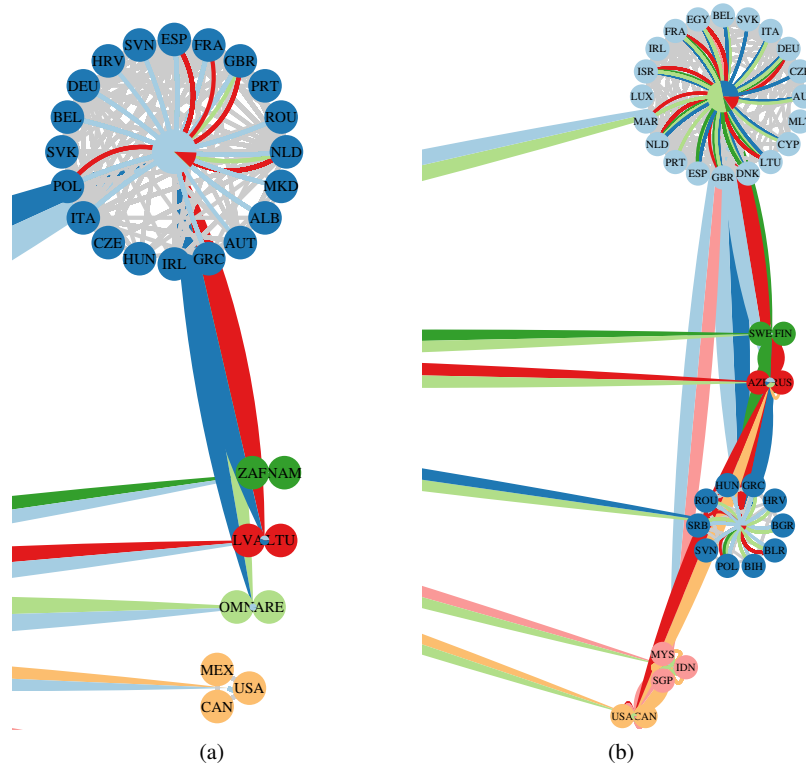


Fig. 1: Clusters for (a) Tomato trade network (b) Potato trade network, where $\Delta = 1000$ and $n = 20$. The colored clusters on the right of both the figures denote the contagion clusters. The rest of the graph is to the left and cannot be seen in this figure in the interest of zooming in on the clusters. The colored edges connect countries belonging to corresponding colored cluster.

work (All13), we observed the formation of clusters spanning multiple continents. When we allowed the clusters to be of any size, we observed one big cluster of size 69. When we limited it to 20 and below, interesting patterns emerged. Perhaps the most extreme of them all is (GTM, CAN, MEX, IND, VNM, ZAF, IDN, USA, NAM) spanning Asia, North America and Africa. A more regional phenomenon that we observe is the breaking up of European countries into two clusters. One cluster consists of EU-T-13 and other European countries merged with some of the North African and West Asian countries such as Israel. The other cluster consists of East European countries and some Arab countries. Clearly, this indicates that if a pest or pathogen is capable of spreading through trade of multiple commodities, then, the expansion can be very rapid and unpredictable. Fortunately, there is no evidence of

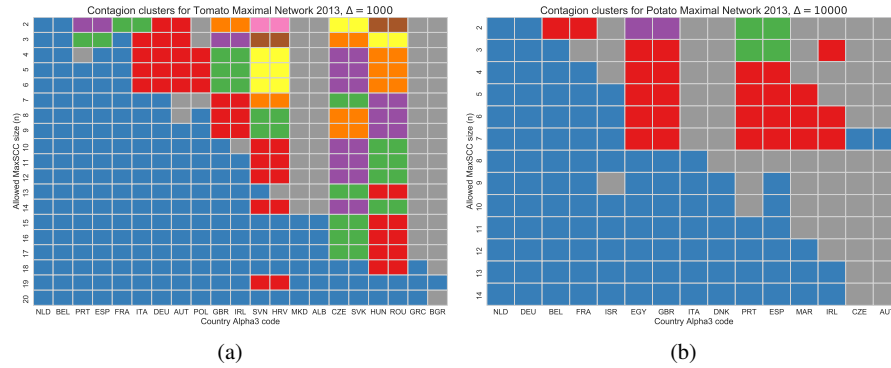


Fig. 2: Clusters for (a) Tomato trade network with $\Delta = 1000$ and (b) Potato trade network with $\Delta = 10000$ and $n = 20$.

T. absoluta having spread through trade of any crop other than tomato. This study also suggests that one should be cautious when aggregating commodities and interpreting the resulting networks.

Cluster size, Step size, probability. Cluster size plays a critical role in discovering important contagion clusters. We have repeated our analysis for step size, $\Delta = 500, 1000$ and 10000 . We observed that as Δ increases, stronger communities remain intact, even though lesser countries are present in the network. When we ran our algorithm with transmission probability, $x = 0.01, 0.1, 0.5$ and restricted the cluster size to be 20 for Tom13, we obtained the same results for the ranked edges and the clusters. This suggests that the clusters are robust to change in probability of transmission.

5 Conclusion and future directions

We analyzed international agricultural commodity networks using the Moore-Shannon network reliability. Under the assumption of a discrete-time SIR diffusion process, we proposed a method to discover highly-connected subsets of vertices, which we refer to as contagion clusters. The method was applied to international trade networks of four crops. We studied the difference in structure of the networks across commodities and across years. We identified important subsets of vertices which can play a key role in the contagion process. There are several obvious directions to extend this work. One important line of work is to study how the cluster structure varies with the underlying diffusion process, such as an SI, SIS model or any other model of the phenomenon being studied. Our multi-graph representation implicitly models the relationship between flow volumes (edge weights) and the infection probability. It would be interesting to know how different functions of edge weights affect mined clusters. In general, a direct implementation of computing edge rank-

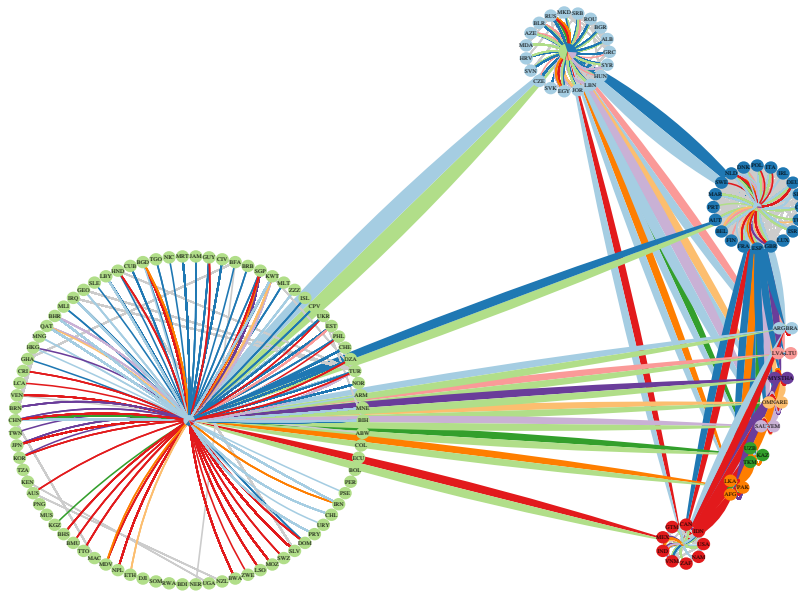


Fig. 3: Clusters for All13 network with $\Delta = 1000$ and $n = 20$. The colored clusters on the right of both the figures denote the contagion clusters. The big cluster on the left represent countries which do not belong to any such SCC. There are 2 big clusters on the right, containing 19 and 20, containing European, African and Middle East Asian countries. The colored edges connect countries belonging to corresponding colored cluster.

ings for weighted graphs will be a significant methodological contribution. Summarizing, the network reliability based methods provide a powerful tool to discover important dynamics-related properties of networks.

References

1. Baskaran, T., Blöchl, F., Brück, T., Theis, F.J.: The heckscher–ohlin model and the network structure of international trade. *International Review of Economics & Finance* **20**(2), 135–145 (2011)
2. Biondi, A., Guedes, R.N.C., Wan, F.H., Desneux, N.: Ecology, worldwide spread, and management of the invasive south american tomato pinworm, *tuta absoluta*: past, present, and future. *Annual review of entomology* **63**, 239–258 (2018)
3. Campos, M.R., Biondi, A., Adiga, A., Guedes, R.N., Desneux, N.: From the western palaeartic region to beyond: *Tuta absoluta* 10 years after invading europe. *Journal of Pest Science* **90**(3), 787–796 (2017)
4. Duch, J., Arenas, A.: Community detection in complex networks using extremal optimization. *Physical Review E* **72**(2), 027,104 (2005)

5. Ercsey-Ravasz, M., Toroczkai, Z., Lakner, Z., Baranyi, J.: Complexity of the international agro-food trade network and its impact on food safety. *PloS one* **7**(5), e37,810 (2012)
6. FAO: Production and trade. <http://www.fao.org/faostat/en/#data> (2016)
7. Ghosh, R., Teng, S.h., Lerman, K., Yan, X.: The interplay between dynamics and networks: centrality, communities, and cheeger inequality. In: Proceedings of the 20th ACM SIGKDD international conference on Knowledge discovery and data mining, pp. 1406–1415. ACM (2014)
8. Hernandez Nopsa, J.F., Daghli, G.J., Hagstrum, D.W., Leslie, J.F., Phillips, T.W., Scoglio, C., Thomas-Sharma, S., Walter, G.H., Garrett, K.A.: Ecological networks in stored grain: Key postharvest nodes for emerging pests, pathogens, and mycotoxins. *BioScience* **65**(10), 985–1002 (2015)
9. Hulme, P.E.: Trade, transport and trouble: managing invasive species pathways in an era of globalization. *Journal of applied ecology* **46**(1), 10–18 (2009)
10. Malliaros, F.D., Vazirgiannis, M.: Clustering and community detection in directed networks: A survey. *Physics Reports* **533**(4), 95–142 (2013)
11. Moore, E.F., Shannon, C.E.: Reliable circuits using less reliable relays. *Journal of the Franklin Institute* **262**(3), 191–208 (1956)
12. Nath, M., Ren, Y., Khorramzadeh, Y., Eubank, S.: Determining whether a class of random graphs is consistent with an observed contact network. *Journal of Theoretical Biology* **440**, 121 – 132 (2018). DOI <https://doi.org/10.1016/j.jtbi.2017.12.021>. URL <http://www.sciencedirect.com/science/article/pii/S002251931730560X>
13. Newman, M.E.: Modularity and community structure in networks. *Proceedings of the National Academy of Sciences* **103**(23), 8577–8582 (2006)
14. Reichardt, J., Bornholdt, S.: Detecting fuzzy community structures in complex networks with a potts model. *Physical Review Letters* **93**(21), 218,701 (2004)
15. Robinson, C., Shirazi, A., Liu, M., Dilkina, B.: Network optimization of food flows in the us. In: *Big Data (Big Data)*, 2016 IEEE International Conference on, pp. 2190–2198. IEEE (2016)
16. Rosenzweig, C., Parry, M.L., et al.: Potential impact of climate change on world food supply. *Nature* **367**(6459), 133–138 (1994)
17. Serrano, M.A., Boguná, M.: Topology of the world trade web. *Physical Review E* **68**(1), 015,101 (2003)
18. Suweis, S., Carr, J.A., Maritan, A., Rinaldo, A., D’Odorico, P.: Resilience and reactivity of global food security. *Proceedings of the National Academy of Sciences* p. 201507366 (2015)
19. Venkatraman, S., Wu, S., Shi, B., Marathe, A., Marathe, M., Eubank, S., Sah, L.P., Giri, A., Colavito, L.A., Nitin, K., et al.: Towards robust models of food flows and their role in invasive species spread. In: *Big Data (Big Data)*, 2017 IEEE International Conference on, pp. 435–444. IEEE (2017)
20. Youssef, M., Khorramzadeh, Y., Eubank, S.: Network reliability: the effect of local network structure on diffusive processes. *Physical Review E* **88**(5), 052,810 (2013)